催化学报
2012 Chinese Journal of Catalysis Vol. 33 No. 11

文章编号: 0253-9837(2012)11-1743-11 国际版 DOI: 10.1016/S1872-2067(11)60448-8 研究论文: 1743–1753

具有{110}面的锐钛矿 TiO_2 单晶的可控合成与光催化性能

吴 谦[1,2], 吴志娇[1], 李永良[2], 高洪涛[3], 朴玲钰[1,*], 张天慧[1], 杜利霞[1]

[1]国家纳米科学中心, 北京 100190

[2]北京师范大学分析测试中心, 北京 100875

[3]青岛科技大学化学与分子工程学院, 山东青岛 266042

摘要: 采用水热法合成了同时具有最高表面能{110}和{001}晶面的锐钛矿 TiO_2 单晶, 通过 X 射线衍射、扫描电镜和激光拉曼光谱等手段对样品的形貌和结构进行了表征, 并系统考察了过氧化氢、氢氟酸和反应温度等关键因素对所得样品中{110}面比例的影响, 实现了持续提高{110}面比例的过程. 在光催化降解亚甲基蓝反应中, 具有{110}面的锐钛矿 TiO_2 单晶的光催化活性显著高于无{110}面的单晶.

关键词: 二氧化钛; 高表面能晶面; {110}面; 水热法; 光催化

中图分类号: 0649 **文献标识码**: A

收稿日期: 2012-07-13. 接受日期: 2012-07-25.

*通讯联系人. 电话/传真: (010)82545653; 电子信箱: piaoly@nanoctr.cn

基金来源: 国家重点基础研究发展计划 (973 计划, 2011CB932802); 国家科技支撑计划 (2011BAK15B05).

本文的英文电子版(国际版)由Elsevier出版社在ScienceDirect上出版(http://www.sciencedirect.com/science/journal/18722067).

Controllable Synthesis and Photocatalytic Activity of Anatase TiO_2 Single Crystals with Exposed {110} Facets

WU Qian[1,2], WU Zhijiao[1], LI Yongliang[2], GAO Hongtao[3], PIAO Lingyu[1,*], ZHANG Tianhui[1], DU Lixia[1]

[1]*National Center for Nanoscience and Technology, Beijing 100190, China*

[2]*Analytical and testing center, Beijing Normal University, Beijing 100875, China*

[3]*College of Chemistry and Molecular Engineering, Qingdao University of Science and Technology, Qingdao 266042, Shandong, China*

Abstract: Anatase TiO_2 single crystals with a high percentage of the high surface energy {110} facets have been successfully synthesized in a simple and economical way using a modified hydrothermal technique in the presence of hydrogen peroxide and hydrofluoric acid. The morphology and structure of the TiO_2 single crystals were characterized by X-ray diffraction, scanning electron microscopy, and Raman spectroscopy. The photocatalytic activity of the TiO_2 crystals for the degradation of methylene blue dye was investigated by ultraviolet light irradiation. The effects of the amounts of HF and H_2O_2 on the morphology of TiO_2 have been studied. The reaction time and temperature have also been investigated. In the TiO_2 single crystals, the {001} and {110} facets are present at the same time. The results indicated that a high yield of single crystals with exposed {110} and {110} facets could be obtained by adjusting the reaction time, reaction temperature, and amounts of HF and H_2O_2. The anatase TiO_2 single crystals with exposed {110} facets showed higher photocatalytic activities than those without.

Key words: titania; facet with high surface energy; {110} facets; hydrothermal technique; photocatalysis

Received 13 July 2012. Accepted 25 July 2012.

**Corresponding author. Tel/Fax: +86-10-82545653; E-mail: piaoly@nanoctr.cn*

This work was supported by the National Basic Research Program of China (973 Program, 2011CB932802) and the National Key Technology R&D Program, Ministry of Science and Technology of China (2011BAK15B05).

English edition available online at Elsevier ScienceDirect (http://www.sciencedirect.com/science/journal/18722067).

作为一种重要的半导体材料, TiO_2 具有光催化活性高、光电化学性质稳定、环境友好、价格低廉

等特性, 广泛应用于环境保护[1]、涂料[2]、传感[3,4]、陶瓷及太阳能电池等领域. TiO_2 有板钛矿、锐钛矿和金红石三种晶型, 其中锐钛矿 TiO_2 在光催化[5~8]和太阳能电池[9~11]等方面表现出优异的性能. TiO_2 的性能不仅与其晶相、尺寸、形貌有关, 还与其外露晶面有关[12,13]. 对于锐钛矿 TiO_2 而言, 不同晶面表面能顺序为 {110} (1.09 J/m^2) > {001} (0.90 J/m^2) > {100} 和 {010} (0.53 J/m^2) > {101} (0.44 J/m^2)[13,14]. 可见{001}晶面的表面能较高, 因而表现出优异的光催化活性[13,14]. 然而在晶体生长过程中, 因体系表面能量最小化趋势而导致高表面能晶面很快消失, 通常难以获得具有高表面能的晶面. 因此, 一般情况下锐钛矿 TiO_2 单晶主要由热力学稳定的{101}面构成. 2008 年, Lu 等[15]以 TiF_4 为原料, HF 为形貌控制剂, 首次制备出具有较高比例{001}面的微米级锐钛矿 TiO_2 单晶. 从此, 制备具有外露高能{001}面的锐钛矿 TiO_2 材料迅速成为研究的热点[16~28].

理论研究证实, 锐钛矿 TiO_2 的{110}晶面的表面能最高[13,14], 但有关其制备的报道很少. 本课题组已首次制备出同时具有{001}面和{110}面的锐钛矿 TiO_2 单晶[29], 但{110}面比例较小. 最近, Pan 等[30]也以 HF 和 $TiOSO_4$ 为原料, 采用水热法制备出{110}面比例较小的 TiO_2 单晶. 本文结合理论计算结果, 系统考察了不同制备条件对所得 TiO_2 样品{110}面及其比例的影响, 采用水热法制备具有高比例{110}面的锐钛矿 TiO_2 单晶, 以期进一步提高其光催化活性.

1 实验部分

1.1 样品的制备

将 0.08 ml 的氢氟酸 (40%, MOS 级纯, 国药集团)、0.01 g 金属钛粉 (99.9%, 200 目, 北京化学试剂厂) 和 27 ml 去离子水依次加入到 100 ml 内衬为聚四氟乙烯的反应釜内, 搅拌下滴加 1.5 ml 过氧化氢 (30%, AR, 北京化学试剂厂). 混合均匀后, 将反应釜密闭并置于烘箱中, 于 150 °C 保持 10 h, 自然冷却至室温. 用去离子水洗涤产物至接近中性, 于 80 °C 干燥 10 h, 600 °C 焙烧 2 h, 得到 TiO_2 单晶样品.

1.2 光催化实验

通过在紫外光区降解亚甲基蓝 (AR, 北京化学试剂厂) 溶液来评价 TiO_2 单晶的光催化活性. 将 0.01 g 催化剂加到 100 ml 含有 10 mg/L 的亚甲基蓝溶液中, 避光搅拌 1 h, 使催化剂与染料之间达到吸附-脱附平衡. 用发射波长为 365 nm 的高压氙灯 (300 W, 北京中教金源科技有限公司) 照射反应器. 在光照过程中, 每隔 15 min 取样, 8000 r/min 离心 5 min, 取上层澄清液在紫外-可见分光光度计 (U-3900, 日本日立) 上进行测试. 亚甲基蓝溶液的浓度对应于 λ = 665 nm 处的吸光度.

1.3 样品的表征

使用日本日立公司 S-4800 冷场发射扫描电子显微镜 (SEM) 观察 TiO_2 样品的形貌. 在日本理学全自动 X 射线衍射仪 (XRD) 上分析样品的物相, 功率 12 W, Cu K_α 靶 (λ = 0.15406 nm), 电压 40 kV, 电流 100 mA, 步长 0.133°. 拉曼光谱 (Raman) 采用 Renishaw Invia plus 型激光拉曼光谱仪测定, 所用波长为 514 nm.

2 结果与讨论

2.1 理论计算

锐钛矿 TiO_2 的高能晶面无法在合成过程中稳定存在, 因此需要引入可以降低其表面能的因素, 以制备出具有高能晶面的样品. 本文利用第一性原理考察 H, B, C, N, O, F, Si, P, S, Cl, Br 和 I 共 12 种元素吸附在{110}晶面上, 对其表面能的降低程度, 采用基于密度泛函理论的平面波超软赝势方法. 在计算不同的表面原子终止结构的体系能量时, 采用广义梯度近似 (GGA) 中的 PW91 方案, 计算中平面波截断能 E_{cut} 均为 380 eV, 自洽精度设置为每个原子收敛至 1.0×10^{-6} eV 以内. 在对结构的优化过程中, 采用 BFGS 算法, 每个原子能量收敛至 2×10^{-5} 以内. 真空层厚度为 1 nm, K 点网格大小为 $2 \times 3 \times 1$. 构建单原子和二聚体模型时, 立方晶胞的 *abc* 都取 1 nm. 优化过程中, 所有原子都是完全弛豫.

图 1 为锐钛矿{110}面吸附不同原子后的表面能数据. 由图可见, F 降低{110}面表面能的能力最强, 稳定效果最佳, 与不同元素稳定锐钛矿 TiO_2 {001}面的结果一致[15].

图 2 为 F^-吸附在锐钛矿 TiO_2 的 (001) 和 (110) 面前后的原子模型图. (001) 面由 5 配位 Ti(Ti_{5C}) 构成, 而 (110) 面由各占 50% 的 Ti_{4C} 和 Ti_{6C} 构成. 引入的 F^-可以与锐钛矿 TiO_2 {001}和{110}面上的

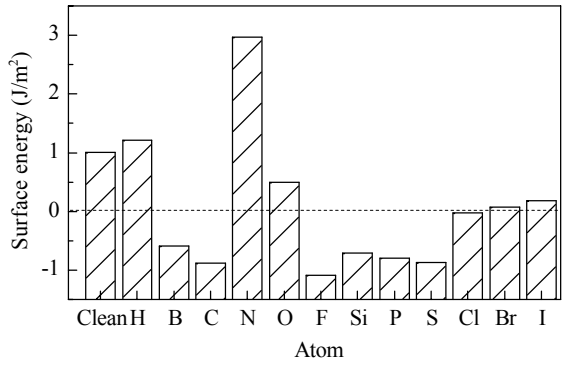

图 1 吸附不同原子后锐钛矿 TiO_2 的 {110} 面表面能

Fig. 1. Calculated energies of the {110} surfaces surrounded by different atoms.

Ti_{4C} 原子结合, 从而极大降低了其表面能. 含 F^- 化学品, 如 HF, 将在锐钛矿 TiO_2 生长过程中降低高能晶面的表面能, 使形成具有{001}和{110}面的锐钛矿 TiO_2 单晶成为可能.

2.2 产物形貌与结构

以 HCl, H_2SO_4 或 HF 为反应物, 进行锐钛矿 TiO_2 单晶的合成, 所得样品见图 3. 有关单晶晶面的确认详见文献[29,30]. 可以看出, 使用 HCl 时, 所制样品{001}面表面能的降低较小, 单晶在[001]轴的方向上较长, {001}面的面积较小, 易生成针状物; 使用 H_2SO_4 时, 生成的单晶粒径较大, 可形成较大比例的{001}和{110}面, 其中后者比较粗糙; 使用 HF 时, 所得单晶同时具有光滑的{001}和{110}面; 而同时使用 H_2SO_4 和 HF 时, 可使样品粗糙的{110}面变光滑. 可见, 该结果证实了理论计算, 即 F^- 对高能面的稳定作用最强.

图 4(a) 为用 HF 制备的 TiO_2 样品的 XRD 谱. 可以看出, 所得样品为结晶良好的锐钛矿型, 其主要衍射峰均与标准卡片 (JCPDS 1-562) 相吻合; 未出现金属钛的特征衍射峰, 表明反应完全. 图 4(b) 为该样品的 Raman 光谱. 由图可见, 样品在 142, 196, 396, 513 和 636 cm^{-1} 处出现典型锐钛矿 TiO_2 特征峰. 这表明所得样品为纯净的锐钛矿相 TiO_2. 本文对不同条件下合成的 TiO_2 单晶进行了 XRD 和 Raman 分析, 证实全部样品均为锐钛矿相.

图 5 为不同 HF 用量制备的 TiO_2 单晶样品的 SEM 照片. 结合我们前期的实验结果可知, TiO_2 产物顶部和底部的两个正方形平面为{001}面[29]; 在 TiO_2 单晶的腰部出现的四个菱形面为{110}面, 与文献一致[30]. 由图可见, 随着 HF 用量的减少, 所得样

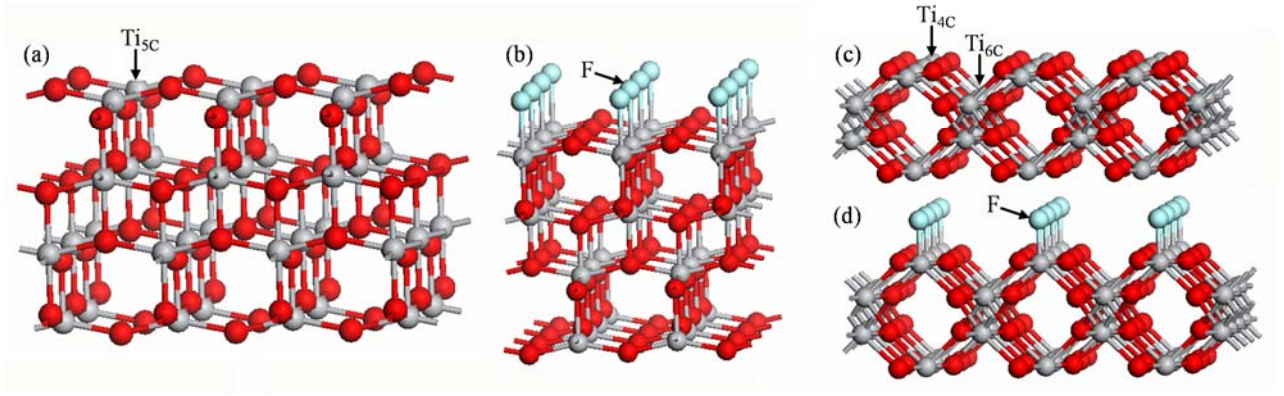

图 2 F^- 吸附在锐钛矿 TiO_2 的 {001} 和 {110} 面前后的原子模型

Fig. 2. Slab models of anatase TiO_2 (001) and (110) surfaces. (a) Unrelaxed (001) surface; (b) F-terminated (001) surface; (c) Unrelaxed (110) surface; (d) F-terminated (110) surface.

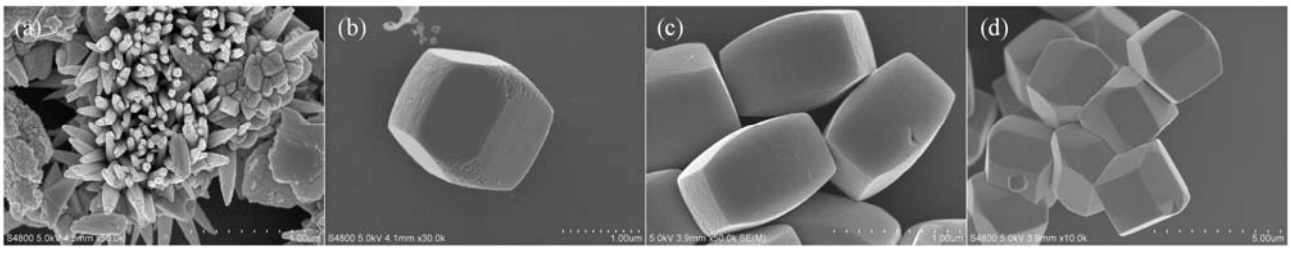

图 3 不同酸制备的 TiO_2 样品的 SEM 照片

Fig. 3. SEM images of TiO_2 crystals synthesized with different acids. (a) HCl; (b) H_2SO_4; (c) HF; (d) H_2SO_4 + HF.

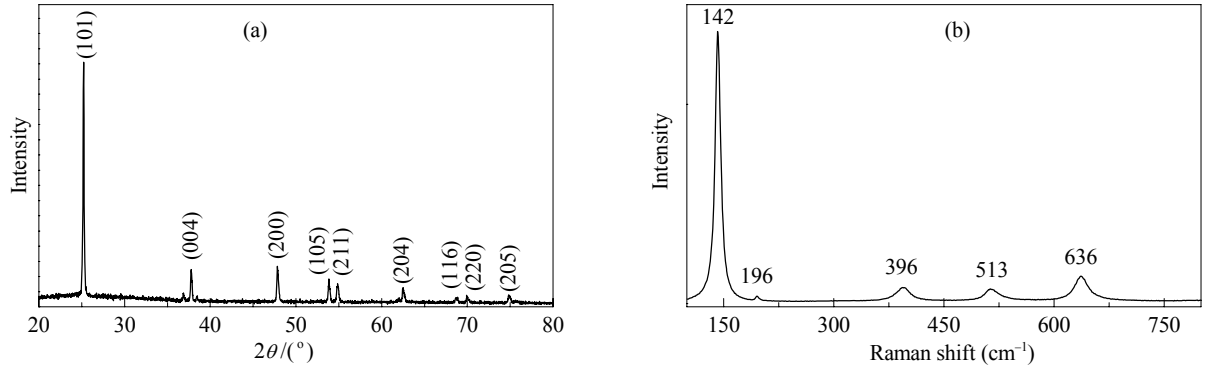

图 4 用 HF 制备的 TiO_2 样品的 XRD 谱和 Raman 光谱

Fig. 4. XRD pattern (a) and Raman spectrum (b) of the TiO_2 single crystals.

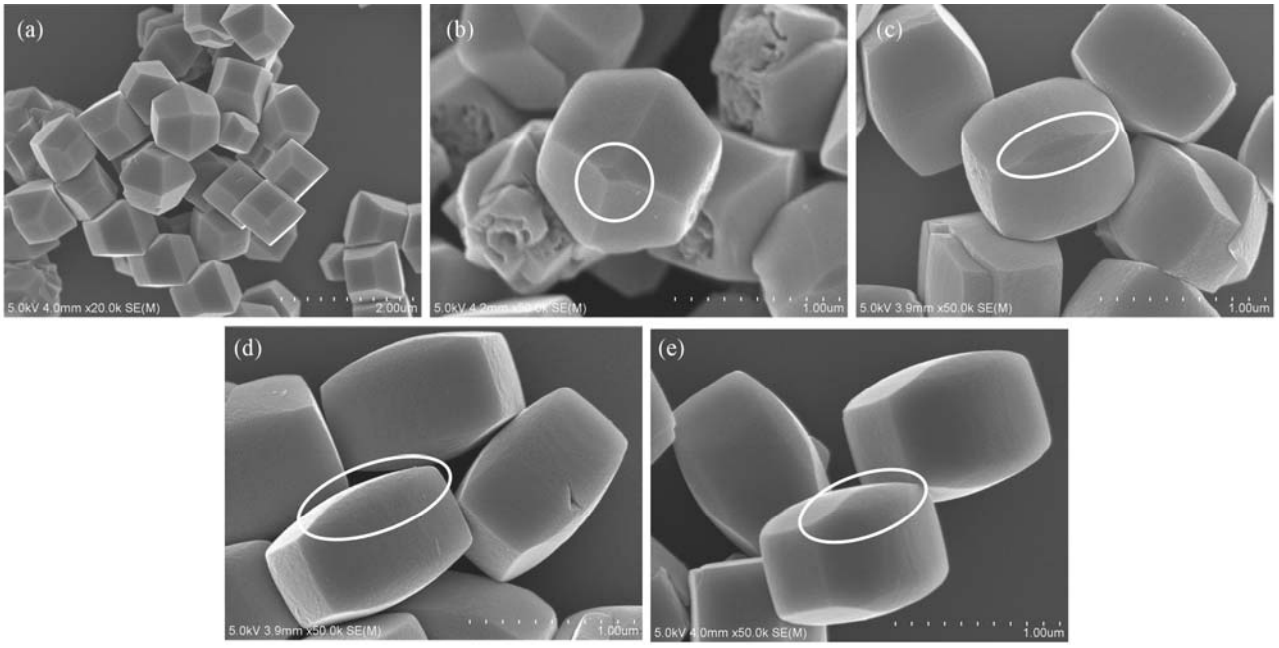

图 5 典型锐钛矿 TiO_2 单晶的 SEM 照片

Fig. 5. SEM images of the TiO_2 single crystals.

晶的{110}面 (圆圈所示位置) 从无到有, 并逐渐增大. 通过控制反应参数, 本文获得了{110}面比例约为 11% 的 TiO_2 单晶 (见图 5(d) 和 5(e)), 与前期结果 (约 4%) 相比显著提高.

由晶体生长热力学的 Wulf 定律可知, 构成晶体平衡外形的晶面到晶体中心的距离与该面的表面能成正比, 而稳定存在的锐钛矿 TiO_2 的{001}和{110}面到达晶体中心的方向互相垂直, 当晶体体积确定时, 一个方向上距离减小, 则另一方向的必定增加. 同时, 与 F 稳定的{110}面的表面能相比, 被 F^-稳定的{001}面的表面能更高[15]. 这意味着 F^-的存在使得所得样品同时具有{001}面和{110}面, 其中{110}面的表面能更低, 因而首先形成. 此时晶体沿[001]向生长为细长型. 然而, 随着 F^-对{001}面的覆盖, {001}面开始稳定出现, 同时抑制了晶体继续沿[001]向的生长. 因此可选择一个平衡点, 使{001}面和{110}面比例达到相对最大. 结果表明, 调控实验参数可获得不同比例{110}面的锐钛矿 TiO_2, 当其比例达到 11% 时, {110} 面沿[001]方向的顶点几乎已与 {001} 面汇合, 达到最大.

上述过程中发生的化学反应如下:

$$Ti + 6HF \rightarrow H_2TiF_6 + 2H_2\uparrow \quad (1)$$

$$H_2TiF_6 + H_2O_2 \rightarrow Ti_2O_5(OH)_\chi \quad (2)$$

$$H_2TiF_6 + 4H_2O \rightarrow Ti(OH)_4\downarrow + 6HF \quad (3)$$

$$Ti(OH)_4 \rightarrow TiO_2 + 2H_2O \quad (4)$$

$$2H_2O_2 \rightarrow 2H_2O + O_2\uparrow \quad (5)$$

下文系统考察了 HF 和 H_2O_2 用量、反应温度及时间等因素对所制样品{110}面形成的影响.

2.3 影响锐钛矿 TiO_2 单晶{110}面比例的因素

2.3.1 HF 的影响

图 6 为不同 HF 用量所制 TiO_2 样品的 SEM 照片. 当 HF 的用量为 0.06 ml 时, 得到的样品交叉生长, 形貌不规则; 至 0.08 ml 时, 样品出现{110}面; 继续增加 HF 用量, F^-对{001}面的稳定作用进一步加强, 单晶沿[001]方向的生长受到抑制, TiO_2 单晶沿[010]和[100]方向生长速度大于[001]方向. 与此同时, 具有最高表面能的{110}面的表面积也逐渐减小, 最终消失.

在锐钛矿 TiO_2 生长过程中, HF 的存在可以降低其{001}面表面能, 从而稳定生长, 形成具有{001}的 TiO_2 单晶[15]. 本文结果进一步表明, HF 的存在还具有稳定最高表面能{110}面的作用. 但当 HF 用量过多时, 其对{001}面的稳定作用高于对{110}面, 从而使{110}面逐渐减小甚至消失. 由{001}和{110}面分子模型图 (见图 2(a) 和 (c)) 可知, 两者分别由 Ti_{5C} (100%) 和 Ti_{4C} (50%) 构成, 由于空间位阻效应的存在, F^-与 Ti_{5C} 的结合比 Ti_{4C} 更容易, 即 F^-更易于稳定{001}面. 当 HF 量过多时, 样品中形成的{001}面比例明显增加, 晶体沿[010]和[100]方向的生长加强, 导致{110}面比例减小.

2.3.2 H_2O_2 的影响

图 7 为 150 °C 下不同 H_2O_2 用量时所制 TiO_2 样品的 SEM 照片. 由图可见, 在无 H_2O_2 或其加入量超过 3.0 ml 时, 得到的样品形状不规则, 交叉严重, 没有{110}面; 当 H_2O_2 加入量为 1.5 ml 时, 所得 TiO_2 单晶的{110}面比例最高.

H_2O_2 可以与 Ti^{4+} 反应生成过氧化钛聚合 $Ti_2O_5(OH)x^{(x-2)-}$ (x = 1~6), 它们可进一步降低 Ti 前驱液的水解速度, 有利于 F^-发挥降低 TiO_2 高能晶面表面能的作用, 也使 TiO_2 单晶有足够时间生长完整, 抑制交叉. 但当 H_2O_2 过多时, 反应产生更多的水 (见式 (5)), 单晶成核的作用增强, 相对而言, 体系中 HF 浓度降低, 使晶体相互交叉现象复现.

2.3.3 反应温度的影响

反应温度对所制 TiO_2 样品形貌的影响如图 8 所示. 可以看出, 当反应温度升高至 150 °C 时, TiO_2 样品结晶完整, 分散良好, {110}面比例较高; 继续升高温度, 单晶颗粒变小, {110}面同比降低, {001}面被腐蚀的程度逐渐严重. 结果表明, HF 酸可以选择性腐蚀{001}面[31,32]. 当温度较高时, 这种定向腐蚀程度增加, 同时影响溶质传质系数, 晶体成核速率变大, 使形成的单晶颗粒变小; 相对而言, 高温有

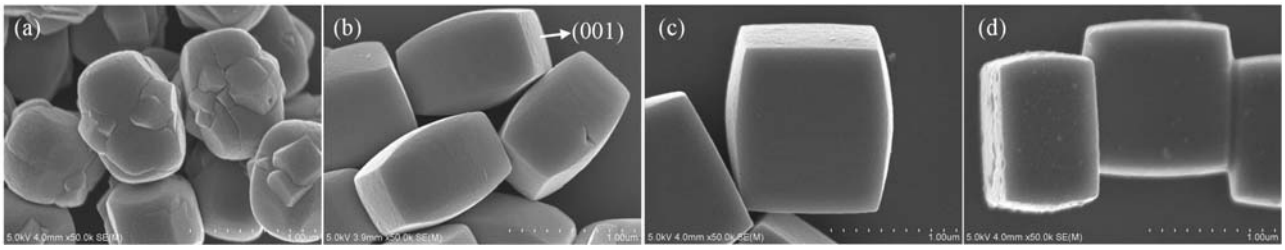

图 6 不同 HF 用量时所得 TiO_2 样品的 SEM 照片

Fig. 6. SEM images of TiO_2 single crystals prepared with different amounts of HF at 150 °C for 10 h. (a) 0.06 ml; (b) 0.08 ml; (c) 0.10 ml; (d) 0.12 ml.

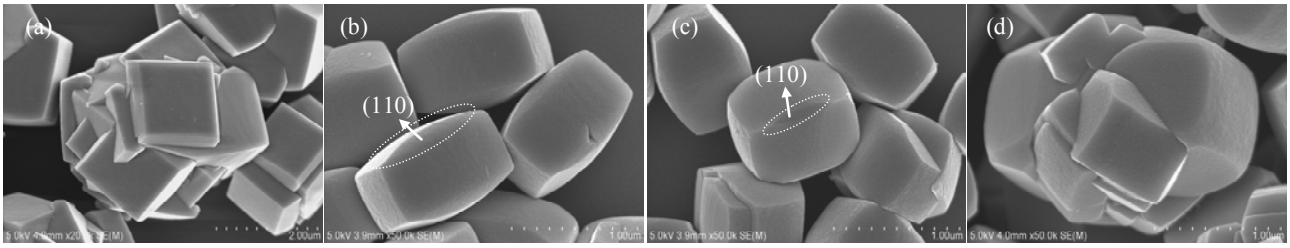

图 7 不同 H_2O_2 浓度时所得 TiO_2 样品的 SEM 照片

Fig. 7. SEM images of TiO_2 single crystals prepared in the presence of different concentrations of H_2O_2 at 150 °C for 10 h. (a) 0.0 ml; (b) 1.5 ml; (c) 3.0 ml; (d) 6.0 ml.

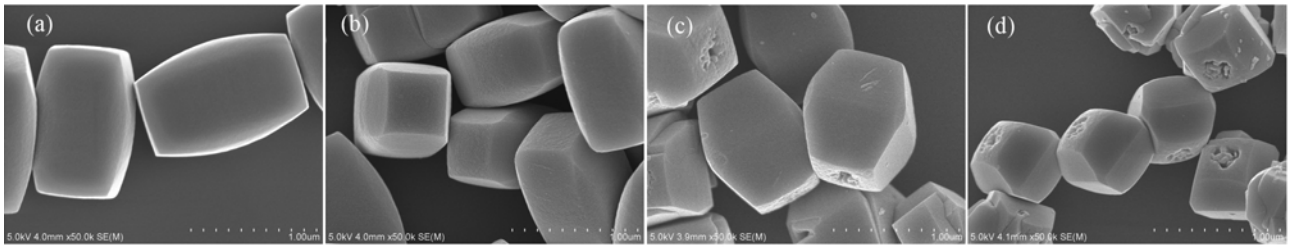

图 8 不同反应温度下所得 TiO_2 样品的 SEM 照片

Fig. 8. SEM images of TiO_2 single crystals synthesized at different temperatures. (a) 140 °C; (b) 150 °C; (c) 180 °C; (d) 200 °C.

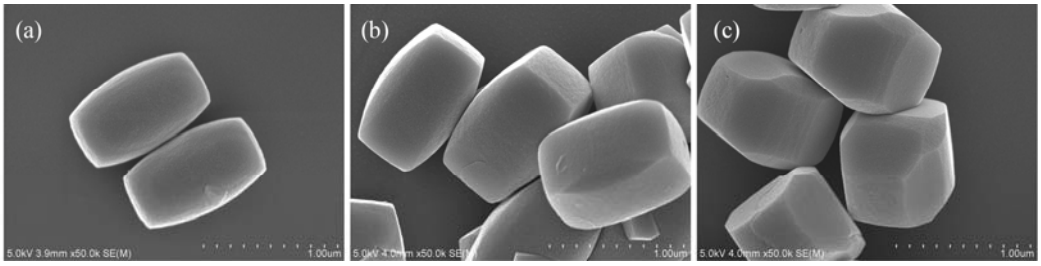

图 9 不同反应时间得到的 TiO_2 产物的 SEM 照片

Fig. 9. SEM images of TiO_2 single crystals synthesized at different reaction time. (a) 3 h; (b) 10 h; (c) 20 h.

利于高表面能晶面的形成, 此时, F^-稳定的{001}面更易形成, 过早地抑制了晶体在[001]向的生长, 使{110}面比例降低.

2.3.4 反应时间的影响

图 9 为反应时间对所制 TiO_2 样品的影响. 反应 3 h 时, 所得 TiO_2 单晶在[001]方向的长度已达到 1 μm, 但其[100]方向的只有 500 nm, 晶体的{101}与{100}面区分不明显, 成圆弧状, 且{110}面未出现; 反应 10 h 时, TiO_2 单晶颗粒在[100]方向的长度可以达到 700 nm, 已经有较大比例的{110}面出现; 至 20 h 时, 样品[100]方向的长度可以达到 800 nm, 而[001]方向的长度基本没有变化, 保持在 1 μm 左右, 各晶面更趋平整, 边界清晰, {110}面比例变化不大.

由此可见, {110}面更易形成而较早出现, 并能一直稳定存在, 晶体沿[001]向生长; 随着反应的进行, F^-的覆盖导致单晶{001}面的表面能降低明显使其稳定出现, 单晶主要沿[010]与[100]方向上生长, 晶体生长逐渐完善, 各晶面间的边界逐渐清晰.

2.4 具有{110}面的锐钛矿 TiO_2 的光催化活性

在测试锐钛矿 TiO_2 单晶的光催化活性前, 样品在 600 °C 焙烧 2 h, 以除去其表面的氟元素及其它吸附物. 图 10 为加入不同催化剂后, 在紫外光照下亚甲基蓝溶液浓度随时间的变化. 由图可见, 与大小相近、各面比例相似的单晶相比, 具有{110}面的

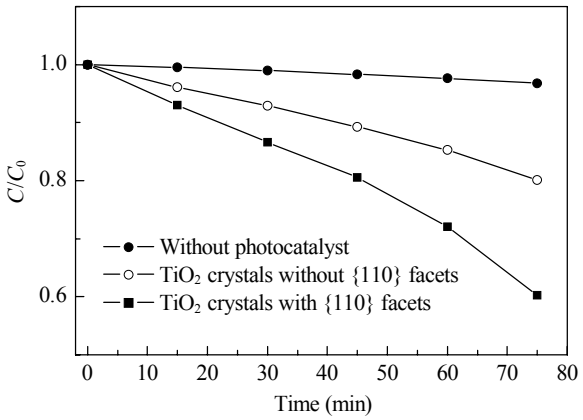

图 10 TiO_2 单晶光催化降解亚甲基蓝的活性曲线

Fig. 10. The photocatalytic properties of TiO_2 single crystals with and without {110} facets for methylene blue (MB) degradation under UV irradiation (MB, C_0 = 10 mg/L).

锐钛矿 TiO_2 单晶比无{110}面的单晶催化降解亚甲基蓝的活性更高, 说明具有最高表面能的{110}面的光催化活性更高, 这为通过形貌控制调节锐钛矿 TiO_2 材料的光催化活性提供了新思路.

本文对比了具有和不具有{110}面的锐钛矿 TiO_2 单晶及 P-25 的比活性 (由反应速率常数 k 与比表面积 A_{BET} 的比值 k/A_{BET} 表示), 结果见图 11. 可以看出, 具有{110}面的锐钛矿 TiO_2 单晶的比活性约为 P-25 的 2 倍, 且明显高于只有{001}面的 TiO_2 单晶.

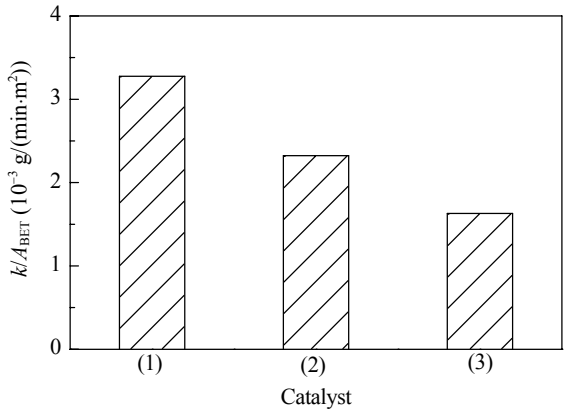

图 11 具有{110}面和无{110}面的锐钛矿 TiO_2 单晶与 P-25 的光催化比活性

Fig. 11. Normalized reaction rate constant (k) per unit surface area (A_{BET}) with different photocatalysts. (1) TiO_2 single crystals with {110} facets; (2) TiO_2 single crystals without {110} facets; (3) P-25.

3 结论

以廉价钛粉为原料, 在不同条件下, 采用水热法可控合成出同时具有{110}和{001}面的锐钛矿 TiO_2 单晶, 验证了理论计算结果. 通过调控 HF 和 H_2O_2 用量以及反应时间和反应温度等参数, 使所得样品中{110}晶面的比例达 11%. 与商用 P-25 和只含{001}面的 TiO_2 单晶相比, 含{110}面的 TiO_2 单晶光催化降解亚甲基蓝的比活性显著提高.

参 考 文 献

1 Bradford M C J, Vannice M A. *Appl Catal A*, 1996, **142**: 73
2 Pfaff G. Reynders P. *Chem Rev*, 1999, **99**: 1963
3 Lin H M, Keng C H, Tung C Y. *Nanostruct Mater*, 1997, **9**: 747
4 Buso D, Post M, Cantalini C, Mulvaney P, Martucci A. *Adv Funct Mater*, 2008, **18**: 3843
5 Linsebigler A L, Lu G Q, Yates J T. *Chem Rev*, 1995, **95**: 735
6 Thompson T L, Yates J T. *Chem Rev*, 2006, **106**: 4428
7 Bahnemann D W, Kholuiskaya S N, Dillert R, Kulak A I, Kokorin A I. *Appl Catal B*, 2002, **36**: 161
8 王后锦, 吴晓婧, 王亚玲, 焦自斌, 颜声威, 黄浪欢. 催化学报 (Wang H J, Wu X J, Wang Y L, Jiao Z B, Yan Sh W, Huang L H. *Chin J Catal*), 2011, **32**: 637
9 Bach U, Lupo D, Comte P, Moser J E, Weissörtel F, Salbeck J, Spreitzer H, Grätzel M. *Nature*, 1998, **395**: 583
10 Grätzel M. *J Photochem Photobiol C*, 2003, **4**: 145
11 肖尧明, 吴季怀, 岳根田, 林建明, 黄妙良, 范乐庆, 兰章. 物理化学学报 (Xiao Y M, Wu J H, Yue G T, Lin J M, Huang M L, Fan L Q, Lan Zh. *Acta Phys-Chim Sin*), 2012, **28**: 578
12 Seker F, Meeker K, Kuech T F, Ellis A B. *Chem Rev*, 2000, **100**: 2505
13 Diebold U. *Surf Sci Rep*, 2003, **48**: 53
14 Lazzeri M, Vittadini A, Selloni A. *Phys Rev B*, 2002, **65**: 119901
15 Yang H G, Sun C H, Qiao S Z, Zou J, Liu G, Smith S C, Cheng H M, Lu G Q. *Nature*, 2008, **453**: 638
16 Zheng Z K, Huang B B, Qin X Y, Zhang X Y, Dai Y, Jiang M H, Wang P, Whangbo M H. *Chem Eur J*, 2009, **15**: 12576
17 Alivov Y, Fan Z Y. *J Phys Chem C*, 2009, **113**: 12954
18 Ma X Y, Chen Z G, Hartono S B, Jiang H B, Zou J, Qiao S Z, Yang H G. *Chem Commun*, 2010, **46**: 6608
19 Zhu J, Wang S H, Bian Z F, Xie S H, Cai C L, Wang J G, Yang H G, Li H X. *CrystEngComm*, 2010, **12**: 2219
20 Zhang D Q, Li G S, Wang H B, Chan K M, Yu J C. *Cryst Growth Des*, 2010, **10**: 1130
21 Chen J S, Tan Y L, Li C M, Cheah Y L, Luan D, Madhavi S, Boey F Y C, Archer L A, Lou X W. *J Am Chem Soc*, 2010, **132**: 6124
22 Liu S W, Yu J G, Jaroniec M. *J Am Chem Soc*, 2010, **132**: 11914
23 Wang X W, Liu G, Wang L Z, Pan J, Lu G Q, Cheng H M. *J Mater Chem*, 2011, **21**: 869
24 Zhang D Q, Li G S, Yang X F, Yu J C. *Chem Commun*, 2009, **29**: 4381
25 蔡陈灵, 王金果, 曹锋雷, 李和兴, 朱建. 催化学报 (Cai Ch L, Wang J G, Cao F L, Li H X, Zhu J. *Chin J Catal*), 2011, **32**: 82
26 向全军, 余家国. 催化学报 (Xiang Q J, Yu J G. *Chin J Catal*), 2011, **32**: 525
27 Lü K L, Cheng B, Yu J G, Liu G. *Phys Chem Chem Phys*, 2012, **14**: 5349
28 Liu S W, Yu J G, Jaroniec M. *Chem Mater*, 2011, **23**: 4085
29 Liu M, Piao L Y, Zhao L, Ju S T, Yan Z J, He T, Zhou C L, Wang W J. *Chem Commun*, 2010, **46**: 1664
30 Pan L, Zou J J, Wang S B, Liu X Y, Zhang X W, Wang L. *ACS Appl Mater Inter*, 2012, **4**: 1650
31 Wang Y, Zhang H M, Han Y H, Liu P R, Yao X D, Zhao H J. *Chem Commun*, 2011, **47**: 2829
32 Xiang Q J, Yu J G, Jaroniec M. *Chem Commun*, 2011, **47**: 4532

英 译 文

English Text

Titanium dioxide (TiO_2) is an attractive material because of its useful properties. It has applications in environmental protection [1], paints [2], sensors [3,4], ceramics, and solar cells. In particular, among the TiO_2 crystalline phases, anatase has proved to be the best in applications such as photocatalysts [5–8] and solar cells [9–11]. Besides its crystallinity, size, and morphology, the exposed surfaces are also important factors that influence the properties of TiO_2

[12,13]. It is well known that the {001} facets are highly reactive, and the average surface energies of anatase are: 1.09 J/m^2 for the {110} facets, 0.90 J/m^2 for the {001} facets, 0.53 J/m^2 for the {100} facets, and 0.44 J/m^2 for the {101} facets [13,14]. Usually high surface energy crystal planes grow quickly and disappear during the crystal growth process because of the minimization of total surface energy. Therefore, anatase TiO_2 single crystals with exposed {001} facets are rarely observed, and anatase is dominated by the thermodynamically stable (101) surface. In 2008, Lu and co-workers [15] synthesized anatase TiO_2 particles with exposed {001} facets by using hydrofluoric acid (HF) as a capping agent under hydrothermal conditions. Since then, several research groups have also prepared anatase TiO_2 single crystals with exposed {001} facets [16–28].

Theoretical studies have demonstrated that the {110} facets of anatase TiO_2 particles has the highest surface energy (1.09 J/m^2) [13,14]. However, the synthesis of anatase TiO_2 single crystals with exposed {110} facets have rarely been reported. In our previous work, anatase TiO_2 single crystals with coexisting {110} and {001} facets were successfully prepared for the first time using a facile and economical route [29]. However, the percentage of {110} facets was relatively low, and the reactivity of the {110} facets was not clear from experimental evidence alone. Recently, Pan and co-workers [30] obtained anatase TiO_2 single crystals with a low percentage of {110} facets via a hydrothermal route. Herein, in combination with the results of theoretical calculations, we studied the influence of the experimental conditions on the synthesis and percentage of {110} facets using a modified hydrothermal technique. TiO_2 single crystals with a high percentage of {110} facets were synthesized and showed enhanced photocatalytic activity compared with naturally occurring anatase for the degradation of methylene blue (MB) dye under ultraviolet (UV) irradiation.

1 Experimental

1.1 Preparation of TiO_2 crystals

The process for the preparation of the samples was as follows. Hydrofluoric acid (40 wt%, 0.08 ml) was placed into a Teflon-lined autoclave containing 0.01 g Ti powder and 27 ml deionized water, and the mixture was stirred vigorously for 10 min. After the addition of 1.5 ml H_2O_2 (30 wt%) to the solution, the mixture was maintained at 150 °C for 10 h. The products were collected by centrifugation, washed with deionized water several times until the pH of the solution was neutral, and then dried at 80 °C in air. Finally, the power sample obtained was heated at 600 °C for 2 h in a static air atmosphere in a furnace to remove the surface fluorine for the measurement of its photocatalytic properties.

1.2 Photocatalysis experiments

The photocatalytic activities of the TiO_2 sample were evaluated by the degradation of MB in a cylindrical quartz flask under UV irradiation (peak wavelength: 365 nm) from a 300 W Xe lamp. Typically, 10 mg of sample was dispersed in 100 ml of the aqueous solution containing 10 mg/L MB, and then the mixture was stirred for 60 min in the dark. The suspension was then exposed to UV light, and a sample was taken every 15 min. The UV-Vis absorption spectra of the samples were recorded after centrifugation at 8000 r/min for 5 min.

1.3 Characterization

The morphologies of the TiO_2 samples were determined using a Hitachi S-4800 scanning electron microscope (SEM). The crystalline structures of the TiO_2 particles were analyzed using a D/Max-TTRIII (CBO) X-ray diffractometer with Cu K_α radiation (λ = 0.15406 nm). Raman spectrum analysis was conducted on a Renishaw Invia plus spectrometer operating at 514 nm.

2 Results and discussion

2.1 Theoretical calculations

To fabricate anatase TiO_2 crystals with high energy surfaces, it is necessary to introduce surface stability factors to reduce the surface energy. Because the high energy surfaces of anatase TiO_2 crystals are not stable during synthesis, we carried out a systematic investigation of 12 non-metallic atoms (H, B, C, N, O, F, Si, P, S, Cl, Br, or I) using first-principle calculations to explore the effects of these adsorbate atoms on the {110} anatase crystal facets. Plane-wave ultrasoft pseudopotentials, which are widely used to study the atomic geometry structure of the bulk and surfaces of materials, were used to calculate the electronic structure. During the calculation of the energy of the system with different surface atomic termination structures, the PW91 scheme of the generalized gradient approximation (GGA) was used. The results indicated that the energy of the truncated plane-wave (E_{cut}) was 380 eV, and the self-consistent accuracy for each atomic was below 1.0×10^{-6} eV. In the process of structure optimization, we used the BFGS algorithm until the energy of each atom was within 2×10^{-5} eV. The vacuum layer thickness was 1 nm, and the K point grid size was $2 \times 3 \times 1$. A cubic unit cell with $a = b = c = 1$ nm was used during the construction of single atoms and two dimer models. All atoms were allowed to fully relax.

In order to find that which kind of atom can effectively reduce the {110} facets energy, we calculated the {110}

facets energies in case of surrounded by different atoms, which are shown in Fig. 1. Figure 1 indicates that adsorption of F atoms gives the lowest surface energy of the {110} facets among the 12 different atoms investigated. In other words, F atoms are the best selection to stabilize the {110} facets of anatase, which is in agreement with previous reports [15].

Figure 2 illustrates the atomic structural models of the clean and F-terminated (001) and (110) surface of anatase. The pure (001) surface has 100% unsaturated Ti_{5C} atoms, while the (110) surface is composed of 50% unsaturated Ti_{4C} atoms and 50% Ti_{6C} atoms. The F atoms can adsorb to the Ti_{5C} atoms on the {001} facets and the Ti_{4C} atoms on the {110} facets, which greatly reduces the surface energies of both surfaces. Thus, chemicals containing F^-, such as HF, can be used to stabilize the high energy {001} and {110} surfaces in the synthesis of anatase.

2.2 Morphology and structure of as-prepared TiO_2

In this work, anatase TiO_2 single crystals were obtained by using different anionic acids as reactants, including HCl, H_2SO_4, and HF. Figure 3 shows SEM images of anatase prepared using different anionic acids. The process of identifying single crystal surfaces of anatase has been described in detail [29,30]. When HCl was used as the reactant (Fig. 3(a)), the surface energy of the {001} facets only slightly decreased, and the growth of single crystals was in the [001] direction. Thus, the surface area of the {001} facets decreased and spicules were easily produced. In the presence of H_2SO_4 (Fig. 3(b)), the {001} facets energy decreased more than with HCl, and the single crystal particles were larger. A larger proportion of {001} and {110} facets were formed, and the {110} facets were relatively rough. When HF was used as the reactant (Fig. 3(c)), the single crystals produced had smooth {001} and {110} facets. When a mixture of H_2SO_4 and HF was used (Fig. 3(d)), smooth {110} facets were obtained. The results confirmed the theoretical calculations that F^- strongly affects the stability of the high energy surfaces of anatase.

Figure 4(a) shows the XRD pattern of the anatase TiO_2 single crystals formed with HF. The synthesized TiO_2 was well-crystallized anatase and the main diffraction peaks in the spectrum were identical with the standard cards (JCPDS 1-562). The reaction was completed as no characteristic Ti diffraction peaks were present. The Raman spectra (Fig. 4(b)) show that the peaks located at 142, 196, 396, 513, and 636 cm^{-1} correspond to the anatase phase. These results indicate that the TiO_2 products were the pure anatase phase. In addition, TiO_2 single crystals obtained under different conditions were also investigated by XRD and Raman, and all were confirmed to be the anatase phase.

Figure 5 shows the SEM patterns of anatase single crystals prepared in the presence of HF. As shown in Fig. 5, the two square planar surfaces at the top and bottom of the TiO_2 crystals are the {001} facets [29], and the four diamond surfaces around the middle of the TiO_2 single crystals are {110} facets, which is in agreement with the literature [30]. From Fig. 5(a) to (e), the percentage of the {110} facets (indicated by circles) gradually increases as the volume of HF is increased. Therefore, by controlling the reaction parameters, TiO_2 single crystals with up to 11% {110} facets can be obtained (Fig. 5(d) and (e)), which is much higher than the previous results (about 4%) [29].

According to the Wulff theory concerning the thermodynamics of crystal growth, the distance from the surface on the crystal to the center of the crystal is directly proportional to its surface energy. The direction from the {001} facets to the crystal center is perpendicular to the direction from the {110} facets. When the crystal volume is fixed, the distance of one direction decreases while the distance of the other direction increases. The {001} facets are stabilized more than the {110} facets by F^- ions [15], with results in the surface energy of the {110} facets being lower than that of the {001} facets in the presence of F^- ions. Thus, the {110} facets form first and the crystal grows faster in the [001] direction and becomes thinner. However, when the {001} facets are terminated by F^- ions, the {001} facets have been stabilized and growth in the [001] direction decreases. This is a contradiction, and only by choosing a balance can the maximum proportion of {001} and {110} facets be obtained. As shown in Fig. 5, anatase with different proportions of {110} facets can be obtained by controlling the experimental parameters. When the percentage of the {110} facets were 11%, the apex of the {110} facets along the [001] direction has almost joined the {001} facets, and the surface area has reached a maximum.

In this paper, the chemical reactions during the experiments are:

$$Ti + 6HF \rightarrow H_2TiF_6 + 2H_2\uparrow \quad (1)$$

$$H_2TiF_6 + H_2O_2 \rightarrow Ti_2O_5(OH)_\chi \quad (2)$$

$$H_2TiF_6 + 4H_2O \rightarrow Ti(OH)_4\downarrow + 6HF \quad (3)$$

$$Ti(OH)_4 \rightarrow TiO_2 + 2H_2O \quad (4)$$

$$2H_2O_2 \rightarrow 2H_2O + O_2\uparrow \quad (5)$$

The influence of some key factors on the formation of {110} facets, including the amounts of HCl and H_2O_2 and the reaction temperature and time, were systematically investigated.

2.3 Effect of the experimental conditions on the percentage of exposed {110} facets of anatase

2.3.1 Effect of HF

The influence of HF concentration on the formation of TiO_2 crystals is shown in Fig. 6. Single crystals were not obtained when the amount of HF was less than 0.06 ml (Fig. 6(a)). When 0.08 ml HF was added, the {110} facets were clearly observed (Fig. 6(b)). As the HF concentration was increased above 0.8 mL, the stability of the F^- adsorbed {001} facets were further stabilized and growth of the TiO_2 crystal in the direction of [001] was inhibited. In contrast, the surface energy of the {110} facets decreased, and the area of the surface decreased and finally disappeared (Fig. 6(c) and (d)).

According to a previous study [15], the {001} facets can be stabilized by HF and anatase TiO_2 crystals containing exposed {001} facets can be obtained in the presence of HF. In this study, the experimental results show that HF not only stabilized the high surface energy {001} facets, but also had a stabilizing effect on the highest surface energy {110} facets. However, when the amount of HF was high, the stabilizing effect of HF on the {001} facets were greater than for the {110} facets, and the {110} facets gradually decreased or even completely disappeared, which is shown in Fig. 2(a) and 2(c). The (001) and (110) surfaces are composed of Ti_{5C} (100%) and Ti_{4C} (50%), respectively. Due to the existence of steric effects, F^- adsorbs easier to Ti_{5C} than to Ti_{4C}. When the amount of HF is high, the percentage of {001} facets increases, and growth along the crystallographic [010] and [100] direction increases, resulting in a decrease of the {110} facets.

2.3.2 Effect of H_2O_2

Figure 7 shows the SEM images of TiO_2 crystals that were synthesized with different concentrations of H_2O_2 at 150 °C. It is clear that the formation of the {110} facets were influenced by the concentration of H_2O_2. In the absence of H_2O_2, or in an amount greater than 3.0 ml, no {110}) facets were observed on the TiO_2 crystals. From Fig. 7(b) and (c), the percentage of {110} facets on the TiO_2 crystals was the greatest when the amount of H_2O_2 was 1.5 ml.

The reaction of H_2O_2 with Ti^{4+} results in the formation of titanium peroxide polymer, $Ti_2O_5(OH)_x^{(x-2)-}$ (x = 1–6). The titanium oxide polymer can further reduce the hydrolysis rate of the Ti precursor, so F^- has more time to stabilize the high energy TiO_2 surfaces, and there is sufficient time for the growth of TiO_2 single crystals, which suppresses the formation of crossed crystals. However, when the amount of H_2O_2 is high, the water in the reaction system is greater (Eq. (5)). Thus, the crystal nucleation effect increases, the concentration of HF decreases, and the crossed crystal phenomenon is observed.

2.3.3 Effect of reaction temperature

A SEM investigation of TiO_2 crystals was performed to gain insight into how the temperature influences the morphology of TiO_2 crystals (Fig. 8). As shown in Fig. 8, the crystallization of TiO_2 was imperfect when the reaction temperature was 140 °C. The morphologies of TiO_2 crystals synthesized at 150 °C were complete, there was a high proportion of the {110} facets, and there was no corrosion. For reaction temperatures greater than 150 °C the crystal size became smaller, the percentage of the {110} facets decreased, and the degree of corrosion of the {001} facets became significant. The results of this and previous studies [31,32] indicate that the {001} facets can be selectively corroded by HF. When the temperature was high, the amount of corrosion increased and the nucleation rate became higher, resulting in the formation of small crystals. In comparison with low temperatures, the high energy surfaces of TiO_2 form more easily at a high temperature. In addition, the {001} facets are stabilized by F^- and are more prevalent on the surface of the crystals, crystal growth in [001] direction is inhibited, and the proportion of the {110} facets decrease.

2.3.4 Effect of reaction time

Figure 9 shows the SEM diagrams of TiO_2 produced after different reaction times. When the reaction time was 3 h (Fig. 9(a)), the length of TiO_2 single crystals in the [001] direction was 1 μm, while the length in the [100] direction was 500 nm. Furthermore, the {101} and {100} facets cannot be clearly distinguished, and the {110}) facets were not observed. When the reaction time was increased to 10 h (Fig. 9(b)), the length of the TiO_2 single crystals in the [100] direction was 700 nm, and there was a larger proportion of {110} facets. For a reaction time of 20 h (Fig. 9(c)), the length in the [100] direction reached 800 nm, while there was no change in length in the [001] direction from the crystals after 10 h.

Furthermore, the crystal surfaces were smoother with clearly defined surfaces, and the proportion of the {110} facets had not significantly changed compared with the crystals after 10 h. Thus, the crystal growth process can be proposed. As the reaction progressed, the surface energy of the (001) surface decreases as it becomes covered by F^-, and a larger proportion of the crystals are {001} facets. The growth of crystals is mainly along the [010] and [100] directions, and, gradually, the growth becomes perfect and the interplanar boundaries become clear.

2.4 Photocatalytic activity of anatase TiO_2 with (110) surfaces

The photocatalysis experiments were carried out with the purpose of determining the potential photocatalytic capa-

bilities of the nanostructures synthesized here. Before applying these crystals to photocatalytic reactions, the surface fluorine atoms were removed by calcining at 600 °C for 2 h. Then, the photocatalytic activities of different catalysts were estimated by measuring the degradation of MB under UV irradiation. As shown in Fig. 10, the anatase TiO_2 single crystals with exposed {110} facets were able to photocatalytically degrade MB, and showed enhanced photoreactivity compared with anatase without exposed {110} facets, but with similar size and proportion of single crystal surfaces.

Through the specific activity, the ratio of the reaction rate constants of k and the specific surface area of A_{BET} (k/A_{BET}), anatase TiO_2 crystals with and without exposed {110} facets can be compared with the TiO_2 P-25 photocatalyst which is a kind of commercial catalyst (Fig. 11). The results indicate that the specific activity of anatase TiO_2 crystal with exposed {110} facets were approximately two times of that P-25, and was significantly higher than that for only {001} facets or without {110} facets.

3 Conclusions

Anatase TiO_2 single crystals with exposed high energy {110} and {001} facets can be obtained using a simple and economical hydrothermal method with guidance from theoretical calculations. The results show that the amounts of HF and H_2O_2, the reaction temperature and time have significant influence on the crystal morphology of TiO_2. By careful control of the reaction parameters, the percentage of exposed {110} facets, which have the highest surface energy in anatase TiO_2 crystal, could be increased to 11%. Moreover, the specific activity of TiO_2 single crystals with an increased proportion of {110} facets in the photocatalytic degradation of MB was significantly higher than for both commercial P-25 and TiO_2 single crystals with only exposed {001} facets.

Full-text paper available online at Elsevier ScienceDirect
http://www.sciencedirect.com/science/journal/18722067